Jet Propulsion Laboratory
California Institute of Technology
4800 Oak Grove Drive
Pasadena, California

GCA Technical Report No. 62-10-G

GEOPHYSICS CORPORATION OF AMERICA
Bedford, Massachusetts

Final Report - Second Phase

For the Period 29 January to 15 November 1962

SPUTTERING ION SOURCE STUDY PROGRAM

CONTRACT NO. 950118

FILE 2628

15 December 1962

TABLE OF CONTENTS

SECTION 1

INTRODUCTION

The first phase of the work consisted in the design, construction and assembly of a novel ion source for solids, whereby the sample is bombarded with an intense beam of fast noble gas ions, which should result in sputtering of the sample material. A certain fraction of the sputtered material was expected to be ionized. The ions can be accelerated and analysed in a mass spectrometer. A final report covering the first phase was submitted to JPL on 28 January 1962.

The second phase of the work, which is now completed, involved the testing of the ion source with particular emphasis on operational performance and applicability to the different types of solids.

SECTION 2

OPERATION OF THE ION SOURCE

2.1 PRIMARY ION BEAM

The Duoplasmatron turned out to be a good choice as a source for the primary ions. Its operation is simple and reliable. Typically, the arc supply voltage between filament and anode is set to 150 V, the magnet current is turned on to 1 amp, and the filament current is turned on and slowly increased until a slight deflection of the arc current meter indicates electron emission which occurs at a filament current of about 9 amp. Then the gas inlet valve is opened slowly until the arc strikes, which results in a sudden drop of the arc supply voltage to a value around 50 volt. The voltage of the baffle-electrode against the filament is then about 30 volt, and the arc current is about 400 ma. The pressure within the duoplasmatron is about 20 microns, and in the target region about 5×10^{-6} torr. Operation of the duoplasmatron under these conditions proved to be optimal with regard to several aspects: The ion extraction hole in the center of the anode plate has a diameter of .008 inches. Due to erosion by the arc, this opening widens up with time, which results in higher gas consumption and an increase of the

pressure in the target region. As a result, flashovers between the anode plate and the ion extraction electrode occur easier at higher pressures.

When the ion extraction opening becomes too wide, the arc will not strike at all, because the pressure in the duoplasmatron cannot build up sufficiently.

The useful life of the extraction opening was several hundred hours when the duoplasmatron was operated under the above conditions, before the anode plate had to be exchanged. Operation at higher arc currents shortens the useful life of the extraction opening considerably, which makes it necessary to replace the anode plate in inconveniently short intervals.

In order to exchange the extraction opening, originally, the duoplasmatron had to be disassembled completely and the whole anode plate which has to be machined with high precision of oxygen free copper had to be replaced. This plate was modified so that now only an inset in the anode plate has to be exchanged, which can be done without disassembling the duoplasmatron.

The gas used for most of the experiments was argon. The gas consumption can easily be calculated. A total ion current of 1 ma drawn by the extraction electrode through the extraction opening corresponds to a flow of 6.25×10^{15} particles/second.. Since 1 cc of gas under standard conditions contains 2.7×10^{19} particles, the gas consumption

amounts to about .0002 st. cc/second. The flow of neutral atoms through the extraction opening during the operation of the discharge is negligibly small. However, if the discharge is switched off only .0001 st. cc/second of neutrals would pass the opening, if the pressure in the duoplasmatron would stay constant. However, this pressure becomes about twice as high under constant flow conditions.

The ion current measured at the target increases proportional with the extraction voltage. It is about 1 ma for an extraction voltage of 15 kv. Above 15 kv frequent flashovers between the extraction electrode and the anode plate make the operation unstable. The size of the focus on the target varies with the voltage of the middle electrode of the einzel lens, and it is smallest when this voltage equals the extraction voltage. Increasing this voltage beyond the extraction voltage does not constrict the focus any more, it only diminishes the intensity, because the effective aperture of the einzel lens becomes smaller.

On the other hand, the size of the focus decreases as the extraction voltage is increased. The smallest focus which can be obtained at 15 kv is a spot of about 3 mm diameter. The size and especially the shape of the focus depend also on the ion beam. When, at a given extraction voltage, the ion current is increased from lower values up to 1 ma by increasing the arc current, then the focus, which is fairly round at low ion current, is distorted and becomes larger. The reason for not achieving a smaller focus is believed to be a space charge effect, and for the distortion of the beam the deflection condenser is suspected to be responsible.

2.2 SECONDARY ION BEAM

The secondary ions sputtered from the target, are accelerated and focused on the mass spectrometer entrance slit by an immersion lens which consists of a short and a long copper cylinder, the latter one being grounded, while the former lies at a potential somewhat lower than the target potential. The correct setting of this potential is signified by a sharp intensity peak behind the entrance slit. The best voltage between the target and the focusing cylinder is about 1/18 of the voltage between target and ground.

Before the mass spectrometer was connected to the ion source, an ion collector with an opening of 1/8" diameter was mounted at the connection port. The total peak intensities of secondary ions were in the order of 10^{-8} amp. The mass spectrometer used is a newly constructed double-focusing instrument, which images the entrance slit stigmatically onto the exit slit. The mass spectrum was obtained by sweeping the target potential simultaneously with the positive plate of the energy-analyser, which is a toroidal condenser, while the magnetic field was kept constant. The collector current was amplified by a vibrating reed electrometer and recorded with an X-Y-Recorder. The X-deflection was proportional to the target potential and therefore the same mass peaks appeared at the same X-positions on the graph paper, independent whether the mass spectrum was scanned upward or downward and independent of the scanning speed. This facilitates the identification of the peaks.

Before each recording of a mass spectrum one particular mass peak was chosen to adjust all parameters for highest ion intensity. A maximum of the collector current can be found by variation of each of the following parameters concerning the primary ion beam: arc supply voltage, solenoid current, einzel lens voltage, deflection plate voltage, and extraction voltage. The appearance of a maximum of secondary ions with variation of the extraction voltage was most surprising, because other investigators have found the sputtering yield to increase always with the energy of the primary ions. The maximum was between 10 and 12 kv extraction voltage.

Parameters concerning the secondary ion beam to be varied for maximum collector current are the immersion lens voltages and the voltage on three pairs of deflection plates, positioned in front of the entrance slit, which are used to guide the secondary ion beam in the right direction through the entrance slit.

SECTION 3

RESULTS

3.1 ANALYSIS OF THE PRIMARY ION BEAM

The composition of the primary ion beam has been analysed in the following way which does not require any mechanical change of the setup. The target has been electrically connected with the anode of the duoplasmatron. Therefore the ions coming out of the duoplasmatron pass the einzel lens and the deflection condenser as usual, although with lower energy, but are then retarded to zero velocity immediately in front of the target. From there on they are subsequently accelerated and focused into the mass spectrometer by the secondary ion optics. Therefore, sweeping the target potential as usual yields the mass spectrum of the ions coming out of the duoplasmatron. Figure 1 shows a typical mass spectrum obtained this way. Besides the large A^{40} peak there are also noticeable the two rare argon isotopes at mass numbers 38 and 36 and a very small amount of doubly charged argon at mass 20. The N_2, O_2 and CO_2 - peaks suggest a small air leak in the duoplasmatron, however, there is also a possibility that the tank argon, which was used for this run, was not quite pure. The water peak is surprisingly small. A small peak at mass 41 has been observed. It cannot be potassium, since there

is no 39-peak nor can it be doubly charged Kr^{82} because the main peak of Kr^{++} should be at mass 42. It is also unlikely to be a hydrocarbon peak, since there are no other hydrocarbons noticeable. Most likely it is an unstable compound AH^{+} which is known to exist in electrical discharges.

3.2 SECONDARY IONS FROM METALLIC SAMPLES

The sputtering experiments were started with randomly picked metals and alloys. The samples were pieces of sheet metal of about 1/4 x 1/2 inch size, which were clamped down to target plate by two steel screws. The surfaces of the samples were not treated in a special way, only washed in acetone. The Figures 2 to 7 show ion spectra obtained from various metals and alloys of regular machine shop purity.

Copper(Figure 2) clearly yielded the two isotopes at mass 63 and 65 in the correct ratio. A sample of brass (Figure 3) gave only the copper isotopes, but not the zinc isotopes. However, the zinc isotopes did appear, when a sample of zinc sheet metal (flashing) was bombarded (Figure 4). It is worth mentioning that other investigators working with low energy (< 1000 volt) bombarding ions never have found secondary zinc ions. On the same trace there are also two copper isotopes and the five nickel isotopes in the correct abundances. Intensive nickel peaks were also obtained from a nickel sample (Figure 5). A sample of stainless steel (304) (Figure 6) yielded the isotopes of Cr, Fe and Ni in the approximate ratio of 30:10:1. An aluminum sample (Figure 7) gave a comparably huge peak of mass 27, about two orders of magnitude bigger than the 63-peak from the copper sample. There also seems to be a

molecular peak Al_2^+ at mass 54, since this peak could not be explained otherwise. The higher sensitivity for aluminum is partially the result of electrical scanning in the mass analyser.

Besides the sample peaks, there are numerous other peaks to be seen on the recordings. A strong peak is usually at mass 23, which can only be sodium, less strong peaks are at masses 24, 25 and 26 in the right ratio of the Mg-isotopes. On all recordings, there is a strong Al-peak at mass 27. It should be mentioned that, when these recordings were made, there was an aluminum inset at the deflection condenser to define the aperture of the primary ion beam. After the experiment with the aluminum sample had shown how easy secondary ions are released from an aluminum surface, this inset was replaced by a copper inset. The edge of the aperture showed considerable erosion. This must have contributed to the aluminum peak on these recordings, and most likely also to the magnesium and sodium peaks, as the mass spectrum of the aluminum sample (Figure 7) suggests.

The 28-peak was originally thought to be N_2^+, but it used to be accompanied by two weak peaks at 29 and 30, noticeable on Figure 3 and, much clearer, on Figures 9 to 13. The relative peak heights of these three peaks indicate that they are Si-peaks. Only once a peak at mass 32 appeared with the Zn sample, right after the system had been vented.

The potassium isotopes at mass 39 and 41 came out very strong from all samples except aluminum, where they are relatively weak.

The peak at mass number 40 was expected to be always the biggest since caused by reflected argon ions. However, it turned out to be usually smaller than the sample peaks. Moreover, in several instances (Figures 9, 10, 11 and 14) it was very small, which suggests the possibility that in those cases where an appreciable large 40-peak has been observed, it might be caused mainly by Ca^+ or maybe MgO^+. On Figure 3 the peaks at mass 40, 42, 43 and 44 appear with peak heights corresponding about to the relative isotopic abundances of Ca. That also confirms the above suggestion. Consequently, since during operation the partial pressure of argon in the apparatus is about two orders of magnitude higher than that of any other background gas, it is very unlikely that any of the other peaks contain appreciable amounts of ions not present in the sample. That must be the case also with the peaks at mass 14 to 18 which appeared in some instances rather strongly.

3.3 SECONDARY IONS FROM INSULATORS

The behavior of samples, which are electrical insulators, turned out to be not different from that of metallic samples. Some difficulties were anticipated with regard to charge-up of the insulator surfaces by the positive primary ion beam. But apparently either secondary electrons released from the mounting plate of the sample, or a fraction of the secondary ions released from the sample, prevent any major potential difference to arise between the sample surface and the mounting plate, to which secondary ion accelerating voltage is applied.

Figure 8 shows an ion spectrum obtained from a piece of limeglass. Remarkably, there are no potassium peaks. The 40-peak is believed to be caused by Ca^+ ions, and not by A^+ ions, because also on the ion spectrum obtained from natural mica (Figure 9) the 40-peak is hardly noticeable. On the other hand, the potassium peaks obtained from mica are extremely strong. The peaks at mass numbers 43 and 44 are probably caused by oxides of aluminum and silicon since these atoms appear very stongly. The ion spectrum of the synthetical product "Supramica" (Figure 10) is quite similar to that of natural mica, only the Al^+ and Si^+ - peaks are less high, and consequently the AlO^+ and SiO^+ - peaks are missing.

Figures 11 to 14 show ion spectra of the rock samples supplied by JPL. All of the expected ions appear in the spectra, although probably the relative intensities of the elements differ from the actual abundance. It should be emphasized that due to the scanning of the accelerating field the ion collection efficiency for the higher masses is much smaller than for the lower masses. This also accounts for the fact that the isotopic abundance ratios of elements with several isotopes seem to be shifted in favor of the lower masses, which is especially apparent with the Mg - and Si-peaks.

The only background peaks appearing with these insulator samples seem to be copper and the constituents of steel, which are the materials of which the duoplasmatron and parts of the primary and secondary ion optics are made.

SECTION 4

DISCUSSION

Although the phenomenon of sputtering is not fully understood, it seems that the ratio of sputtered ions to sputtered neutrals can be expressed by the Langmuir-Saha formula:

$$N^+/N^O = \exp(11606(W-I)/T)$$

where

N^+ = number of positive ions

N^O = number of neutrals

W = work function of surface

I = ionization potential of particle

T = temperature of surface in ^OK

This formula actually applies to thermal ionization on hot surfaces. In the case of sputtering the temperature T represents a highly localized "apparent temperature" being much higher than the bulk temperature of the sample, which is kept in our case around room temperature by cooling in order to prevent evaporization.

If the ionization potential of the particle is lower than the work function of the surface, then the exponent is positive and practically all particles come off in ionized form, independent of the temperature. This is usually the case with alkalis evaporating from a surface other than their own.

However, if the ionization potential of the particle is higher than the work function of the surface, than the exponent is negative, and the fraction of ionized particles depends very strongly on the difference of those two figures. For pure zinc for instance, the difference is $I - W = 9.39 - 4.27 = 5.12$ ev, whereas for pure Aluminum it is only $5.98 - 4.20 = 1.78$ ev. This accounts for the fact that the Al-ions appeared so much stronger than the Zn-ions. One way to find the actual "apparent temperature" would be to compare the amount of sputtered ions with the amount of sputtered neutrals. No provision for such a measurement is made in the present setup. However, from the recorded ion intensities a rough estimate of the "apparent temperature" existing under the conditions of the measurements can be made. Assuming equal total sputtering yield for any two elements, and also constant sensitivity of the mass spectrometer, one can write down the above formula for the two elements and eliminate the temperature T, which is assumed to be the same in both cases. Doing this with the ion intensities obtained from Al, Ni, Cu and Zn we arrived at an average "apparent temperature" of about $5000^{\circ}K$.

One more look at the Langmuir-Saha formula tells us that in the case, where the ionization potential I is larger than the work function W, the

fraction of ionized particles increases with the temperature. For infinite temperature the ratio would become unity, which means, that as many particles would come off the surface in ionized form as in neutral form, independent of the difference between ionization potential and work function. Therefore, the discrimination between different elements becomes smaller if the "apparent temperature" can be made higher. It is very likely that this "apparent temperature" increases with either the energy or the momentum of the primary ions. It is known that the total sputtering yield increases with the momentum of the primary ions. The question whether the energy or the momentum is the deciding factor for the "apparent temperature" could be determined by using argon ions of higher energy and also some heavier noble gas ion of the same energy.

The discrimination between different elements due to different total sputtering yields comes also into the picture, but seems to be by far not as severe as the discrimination effect described above.

One point worth consideration is the question if the formation of surface layers could play a role. The primary ion beam of 1 ma intensity covering a spot of 3 mm diameter on the target corresponds to a bombardment rate of roughly 6×10^{16} particles/cm^2 sec. The average distance between the atoms on the surface of the sample is about 10^{-8} cm, which gives an area density of 10^{16} particles/cm^2. Since it can be assumed that on the average each bombarding particle deliberates one particle from the surface, one can conclude from these figures that it takes only about two tenths of a second to remove a monolayer from the surface. On

the other hand, at a background pressure of 10^{-5} torr, the number of gas particles, which hit the sample surface, is roughly 3×10^{15} particles/cm^2 sec. This is by a factor 20 less than the bombardment rate of the primary ion beam, which means that the formation of any surface layer on the sample due to the background gas can not compete with the removal of particles from the surface. All original surface layers are quickly removed by the primary ion beam, which thereafter bombards the clean surface of the sample.

SECTION 5

CONCLUSION

The sputtering ion source for the analysis of solids, which has been built during the first phase of the contract, has been tested thoroughly during this second phase of the contract. Much valuable experience has been collected about what improvements could be made in the direction of increasing the ion yield and diminishing the discrimination effects.

One surprising and very valuable feature of the new ion source is that the gaseous background from hydrocarbons and the constituents of the air seem to be negligibly small compared to the intensities of the sputtered ions. The mass spectra are extremely simple and consist essentially only of peaks from single ionized atoms.

Another unique feature of the ion source as compared to the conventional spark source is its stable operation, which permits electrometric recording of the mass spectrum.

It can be stated, that the results are very encouraging and it looks, as if this novel ion source could become a unique tool for solids analysis, applicable to conducting and insulating materials as well.

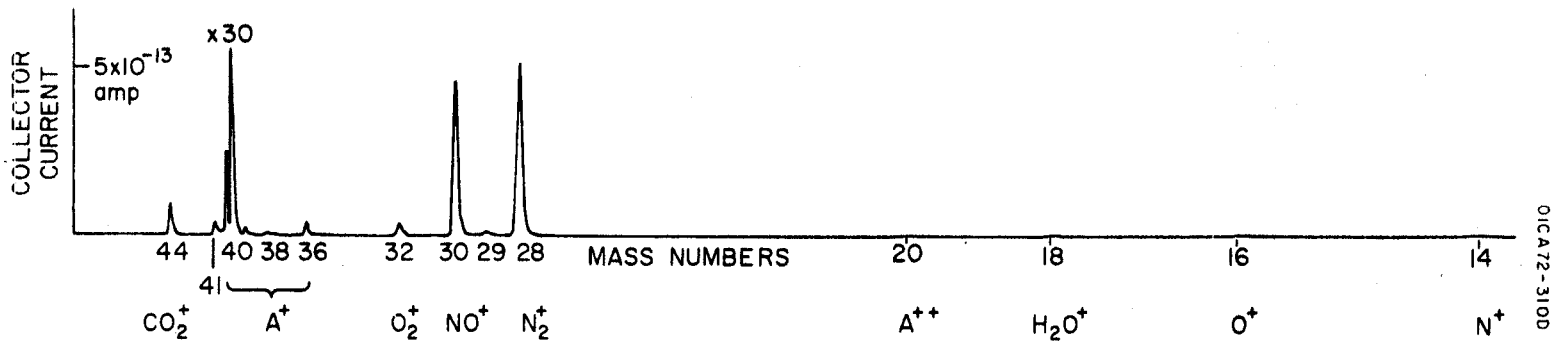

FIGURE 1
MASS SPECTRUM OF THE PRIMARY ION BEAM

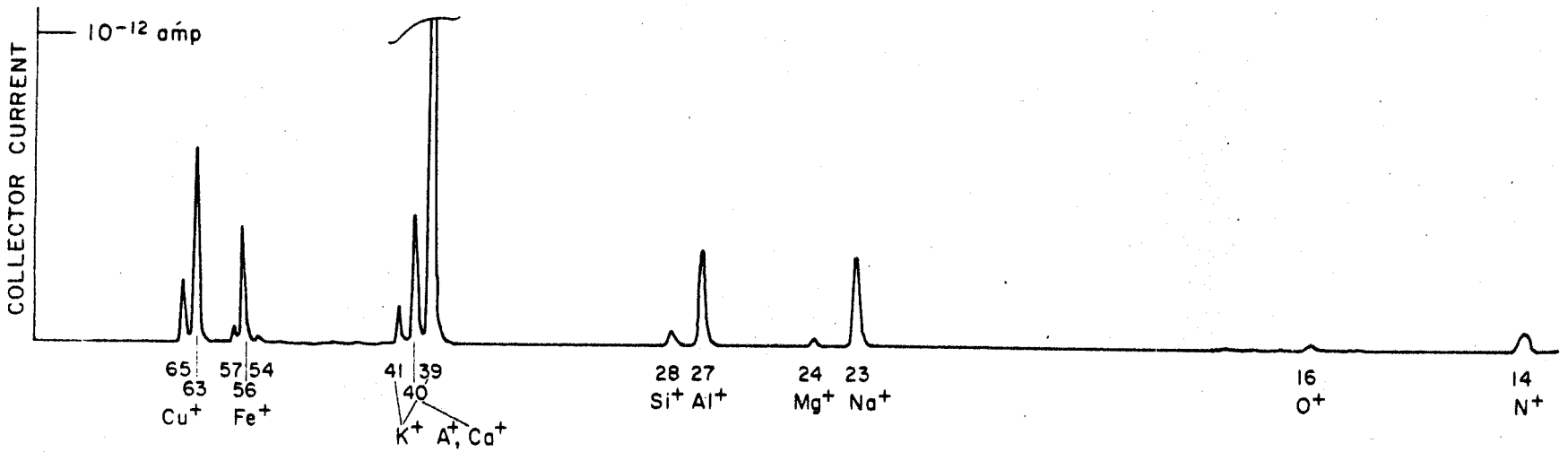

SECONDARY ION SPECTRUM OF A COPPER SAMPLE

Figure 2.

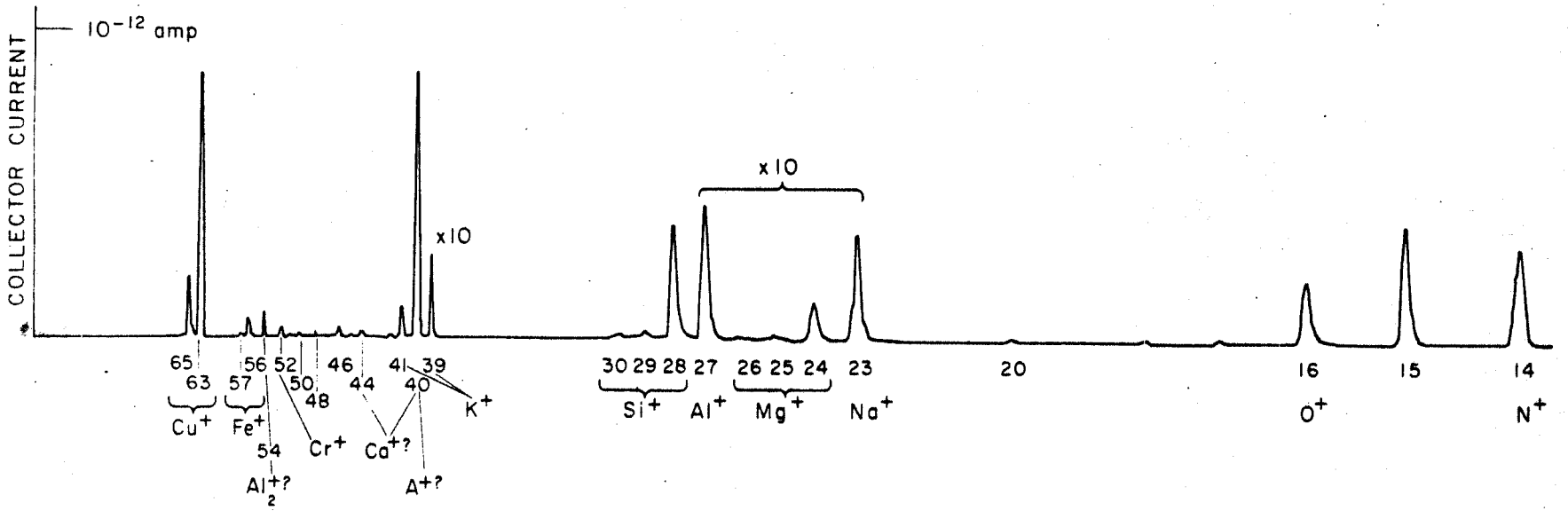

SECONDARY ION SPECTRUM OF A BRASS SAMPLE

Figure 3.

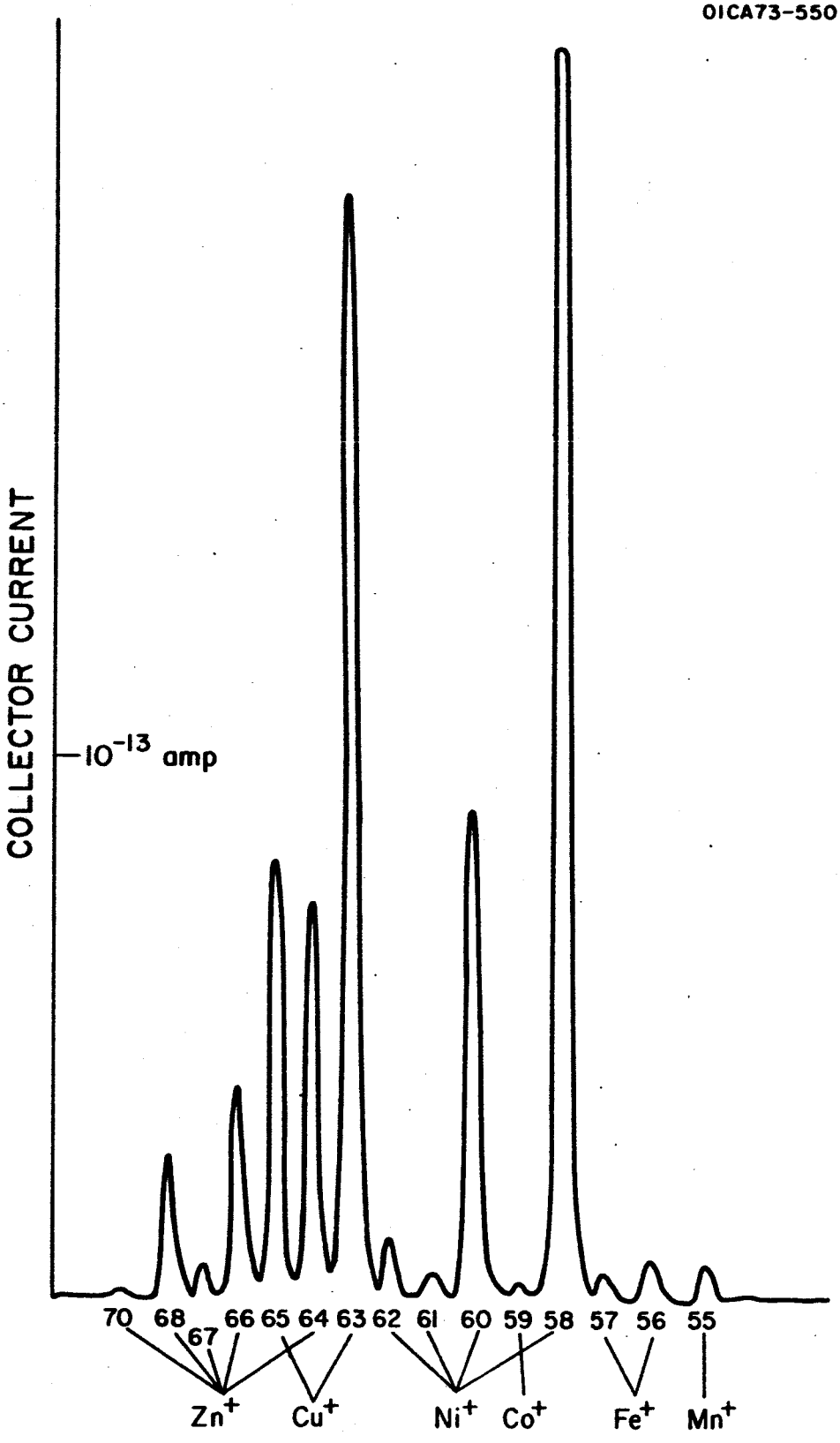

SECONDARY ION SPECTRUM OF A ZINC SAMPLE

Figure 4.

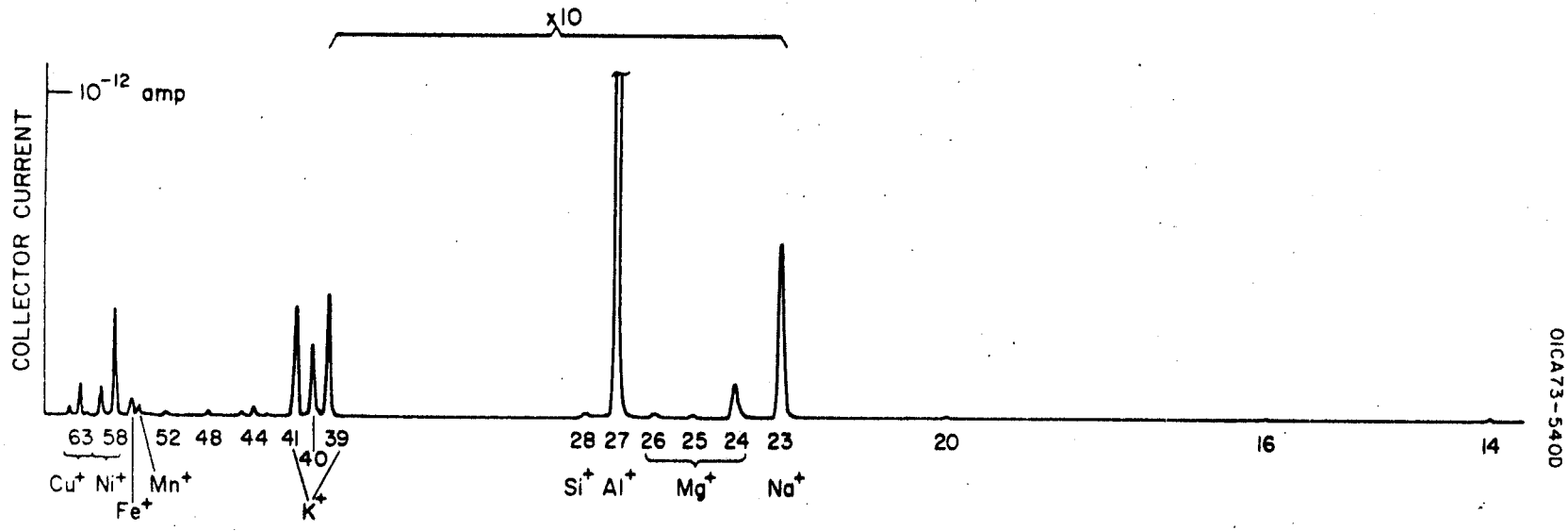

SECONDARY ION SPECTRUM OF A NICKEL SAMPLE

Figure 5.

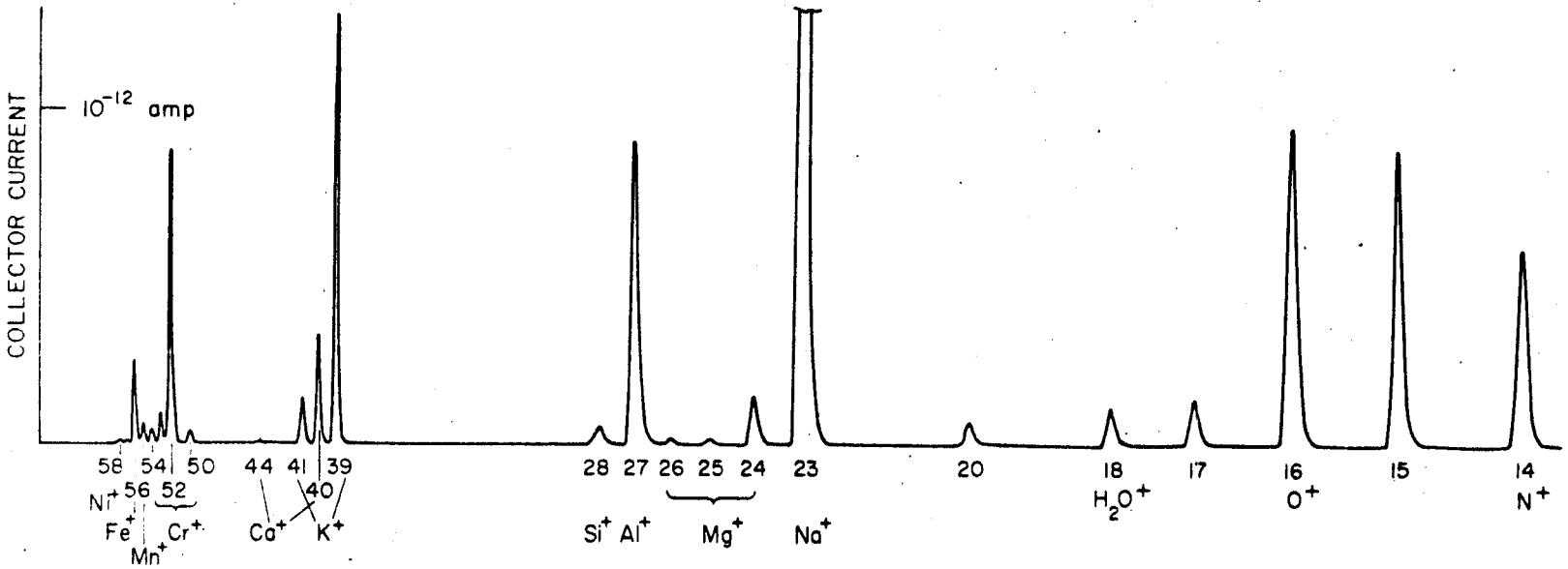

SECONDARY ION SPECTRUM OF A 304 STAINLESS STEEL SAMPLE

Figure 6.

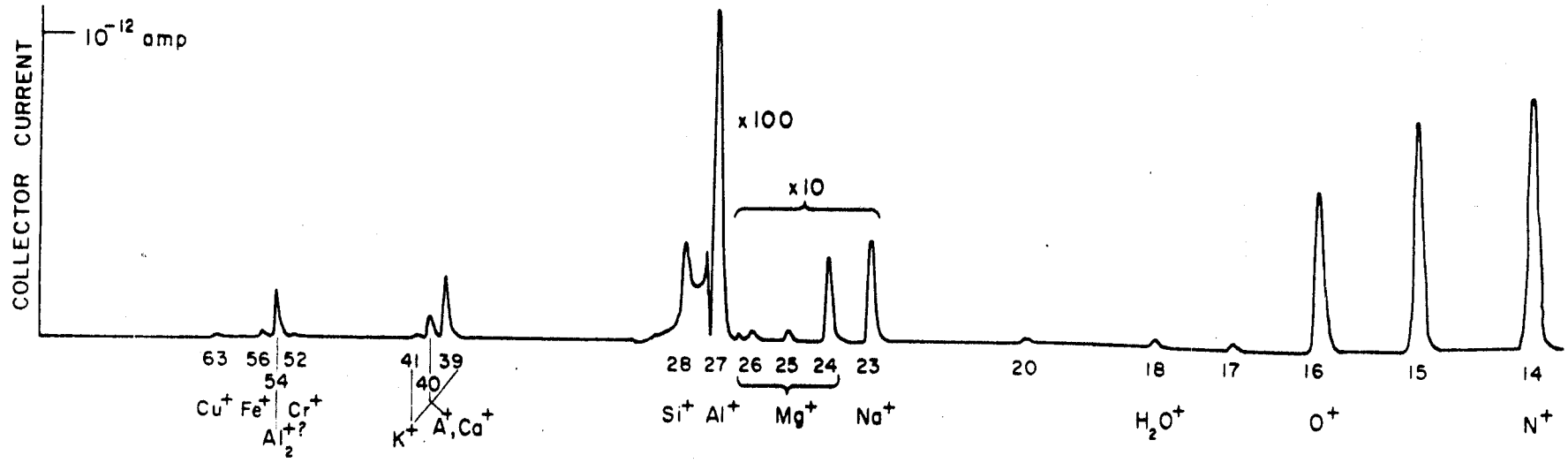

SECONDARY ION SPECTRUM OF AN ALUMINUM SAMPLE

Figure 7.

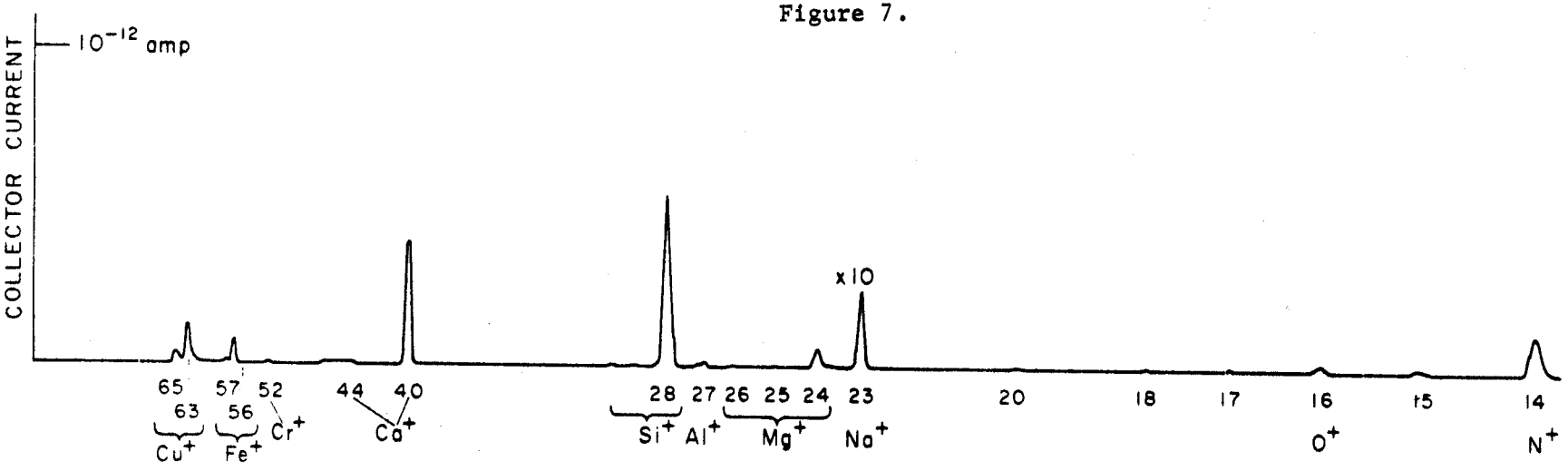

SECONDARY ION SPECTRUM OF LIMEGLASS

Figure 8.

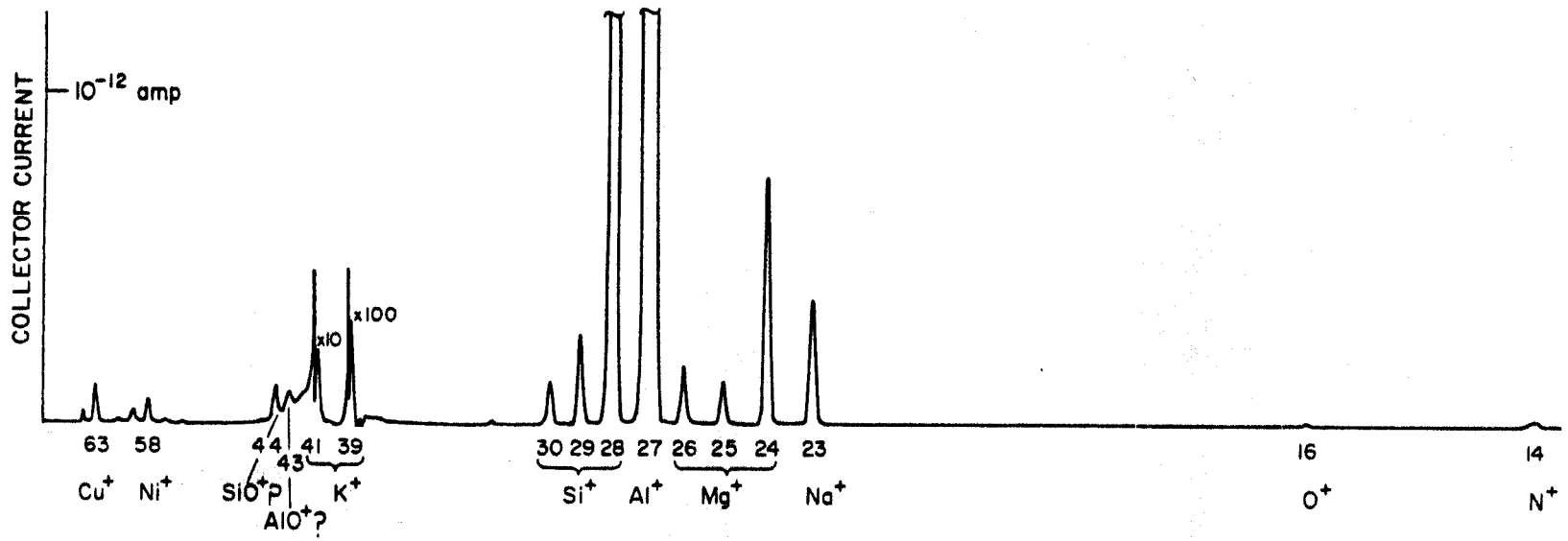

SECONDARY ION SPECTRUM OF NATURAL MICA

Figure 9.

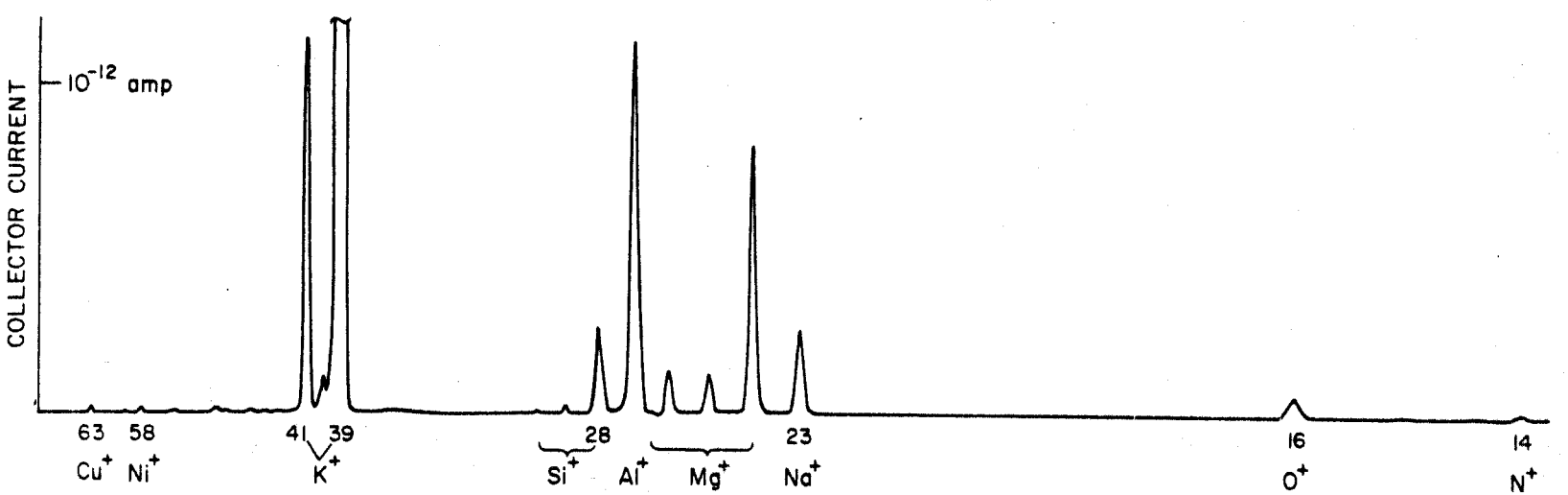

SECONDARY ION SPECTRUM OF SUPRAMICA

Figure 10.

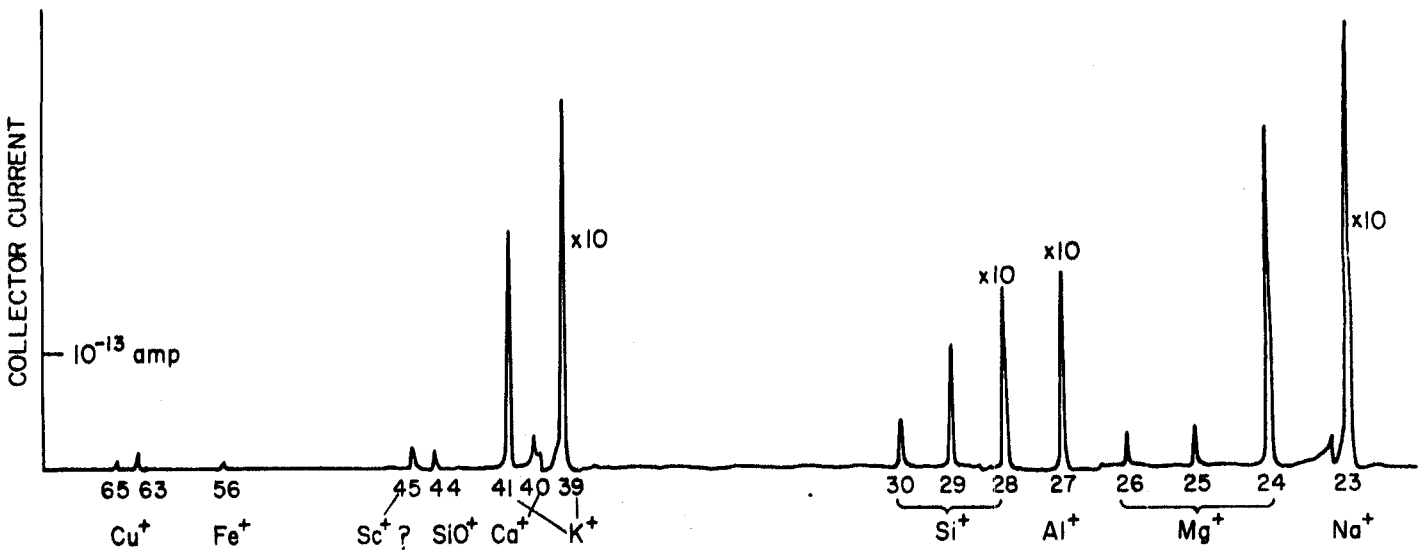

FIGURE 11. SECONDARY ION SPECTRUM OF QUARTZ MONZONITE

IONS EXPECTED: Na, Mg, Al, Si, K, Ca, Fe

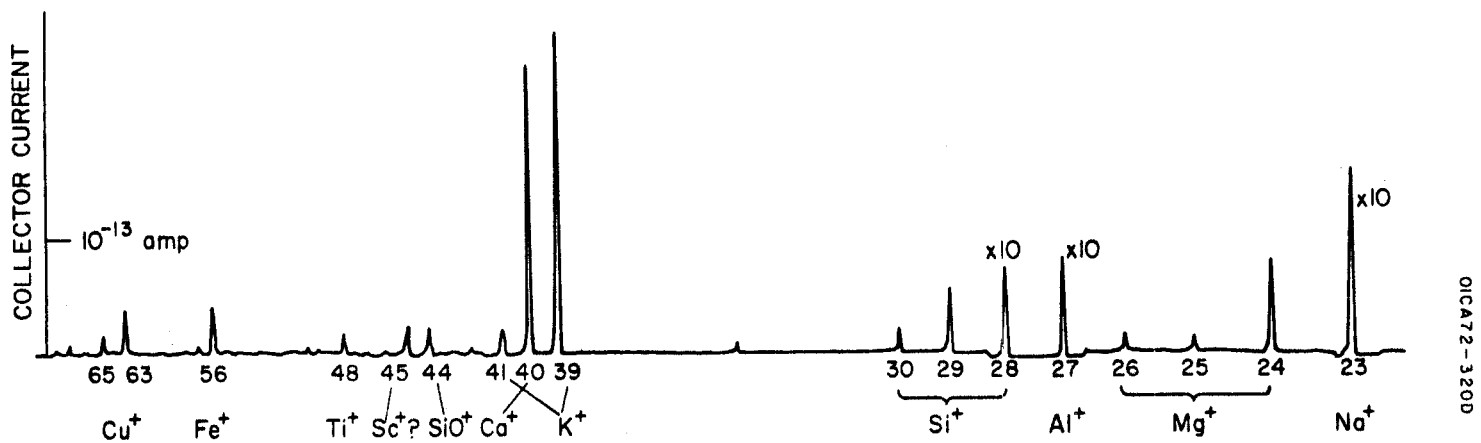

FIGURE 12. SECONDARY ION SPECTRUM OF HORNBLENDE

IONS EXPECTED: Na, Mg, Al, Si, K, Ca, Ti, Fe

01CA72-320D

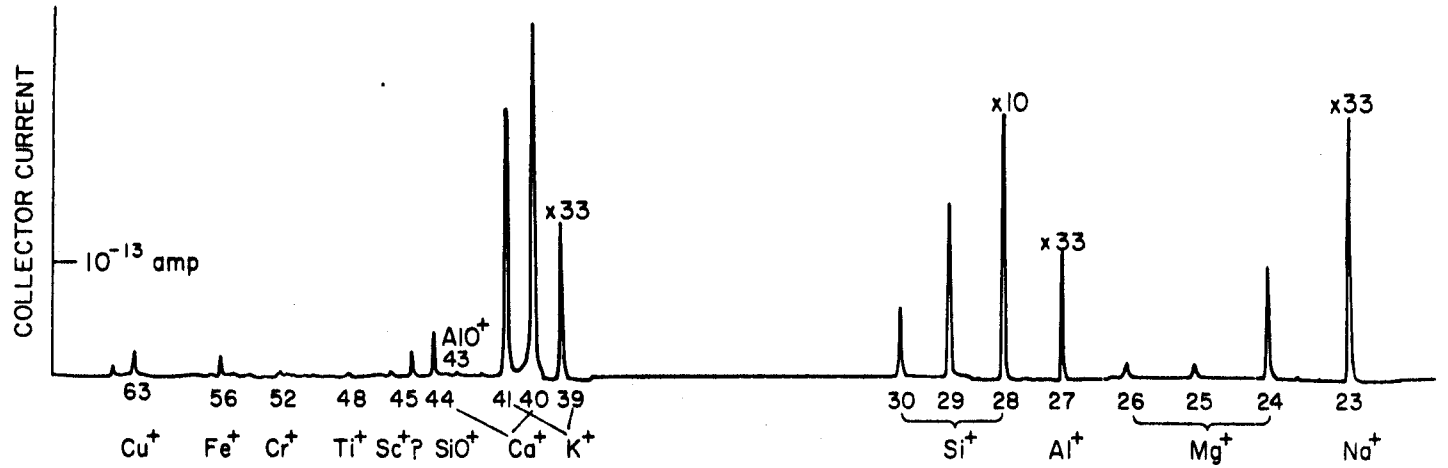

FIGURE 13. SECONDARY ION SPECTRUM OF GRANITE FROM VERMONT

IONS EXPECTED: Mg, Al, Si, K, Fe

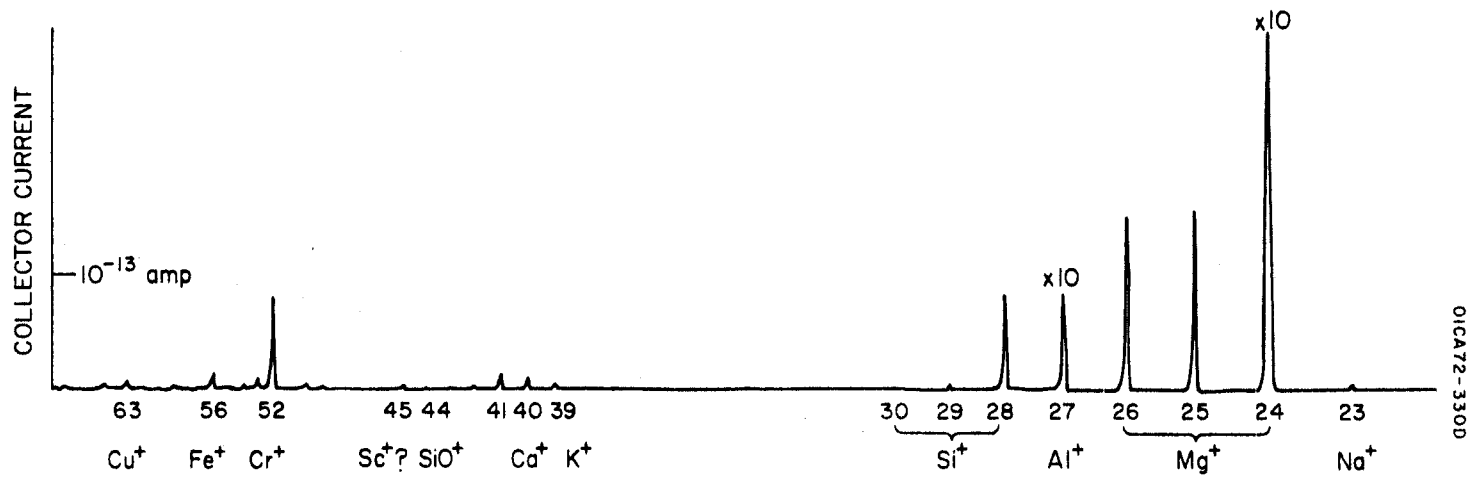

FIGURE 14. SECONDARY ION SPECTRUM OF DUNITE WITH CHROMITE

IONS EXPECTED: Mg, Si, Cr, Fe